

Growth of anchorage-dependent mammalian cells on microstructures and microperforated silicon membranes

E. RICHTER, G. FUHR, T. MÜLLER, S. SHIRLEY

Humboldt-Universität zu Berlin, Institut für Biologie, LS Membranphysiologie, Invalidenstr. 43, 10115 Berlin, Germany

S. ROGASCHEWSKI

Humboldt-Universität zu Berlin, Institut für Physik, LS Oberflächenphysik und Atomstoßprozesse, Invalidenstr. 110, 10115 Berlin, Germany

K. REIMER, C. DELL

Fraunhofer-Institut für Siliziumtechnologie ISiT, Dillenburger Straße 53, 14199 Berlin, Germany

Anchorage-dependent cells (mouse fibroblasts L929 and 3T3) were cultivated on microstructures made by semiconductor technology. Both cell lines showed normal growth on silicon surfaces covered with microelectrode arrays as well as on microperforated silicon membranes with square pores made by anisotropic etching (5, 10 or 20 μm edge length at the top and 1.2, 6.2 or 16.2 μm at the bottom). The cells spread over the 5 and 10 μm pores, but mostly failed to cover the 20 μm ones. They were able to cross the silicon membrane through the pores and to grow and spread on the under side of the membrane. Small pores (about 1 μm^2) impeded but did not prevent cells crossing the membrane. Medium and large pores were freely crossed. Negative dielectrophoresis was used to achieve accurate positioning of cells above pores or to repel them from the chip surface (a.c., square wave, 2.5 V peak-to-peak, 5 MHz). The results are discussed with respect to their microtool applications for single-cell technologies.

1. Introduction

Many vertebrate cells cultured *in vitro* are "anchorage dependent" and require a substrate upon which they can grow and divide. Commonly used substrates for these cells are glass and negatively charged polystyrene or other plastics with specially prepared or coated surfaces. Materials such as palladium, stainless steel and other metals have been tested. Recently, semiconductor materials like silicon and its oxides have become relevant for animal cell culture as microstructures produced by semiconductor technology offer outstanding possibilities for the handling and monitoring of cells, especially single cells.

Microstructures and microstructuring techniques have been used to guide cells by micropatterns of differential adhesiveness [1–5], to study the effects of topographic cues (steps and grooves) on cell guidance [6–10] and to simulate three-dimensional tissue-like systems [11]. Microstructures have also been used for monitoring electrogenic cells in culture [6, 10, 12–14] and for the detection of cell motility and adhesion processes [15, 16].

In our laboratory, microstructures have been used in single-cell dielectric spectroscopy and as cell traps and manipulators utilizing high frequency electric

fields [17]. This work has been done with freely suspended cells. The ability of anchorage-dependent mammalian cells to grow on our semiconductor structures must be demonstrated before we can adapt these techniques.

Recently a combination of impedance and noise analysis using microelectrode systems has been presented [18, 19]. If the electrodes are small enough, any cell motion (movements in the nanometre range), cell adhesion process or cell–cell interaction can be detected by the electric current between the electrodes. Measurements have been made with confluent cell layers as there is only a small shunt pathway around cells. Embedding cells in the pores of a polycarbonate filter also reduces the shunt current and allows an increase in the sensitivity of cell impedance spectroscopy [20].

We would expect similar effects if a microperforated silicon membrane is used instead of a filter. Such membranes have the advantage that the numbers and the positions of the holes can be adjusted to develop special cell sensing devices. If cells growing on perforated membranes were able to cover the holes, passive electric properties should be measurable. Motion over the surface and cell–cell interactions should produce

quantitative electrical signals. With microelectrode arrays this may be possible at the single-cell level. The design of optimal structures with individually addressable micropores requires information about the growth behaviour of cells on perforated silicon membranes.

We need to deposit cells accurately over the holes. Possibly, this can be done by means of microfabricated three-dimensional field cages [17, 21]. Inhomogeneous fields either attract cells to a high-field region (positive dielectrophoresis) or repel them from it (negative dielectrophoresis). Whether attraction or repulsion occurs depends on the field frequency and the passive electric properties of the cell and surrounding medium [22]. The use of repulsive forces protects the cells from extremely high-field regions and other troublesome effects at the electrode surfaces. If the effective permittivity or the conductivity of the cell is smaller than that of the surrounding solution, there is a frequency above or below which negative dielectrophoresis occurs [23]. For living cells suspended in culture medium, both permittivity and conductivity are lower than that of the solution and negative dielectrophoresis is found over the whole frequency range (Hz to GHz). In the case of most animal cells, the conductivity of the cytoplasm ranges between 0.1 and 0.6 S/m and the permittivity between 30 and 60. By comparison, typical culture media have conductivities of 0.6 to 2 S/m and permittivities up to 70 [24]. We have shown [25] that it is possible to cultivate adherently growing fibroblasts (3T3, L929) under the prolonged application of a field large enough to manipulate cells. Fields of 50 kV/m had no marked influence on cell viability, morphology or motility for periods of up to 3 days. Consequently, negative dielectrophoresis is a possibility for positioning cells on a perforated membrane. Electrodes arranged on narrow bridges might repel suspended cells and allow their settlement only at the holes. However, little is known about the behaviour of adherently growing cells on electrode arrays and surfaces structured in the micrometre and submicrometre range.

In this study we investigated the following questions:

- How do fibroblasts grow on microstructures used for cell trapping, characterization and manipulation?
- How does a perforated silicon surface have to be structured so that fibroblasts can cover the pores?
- Are fibroblasts actively able to cross small pores with sharp edges?
- How must electrode arrays be designed to prevent anchorage of fibroblasts on a silicon surface?

2. Materials and methods

2.1. Fabrication of microstructures

2.1.1. Microelectrode arrays

Microelectrode arrays were fabricated using different substrate and electrode materials. Platinum electrodes on Si-wafer and gold electrodes on Si-wafer and Pyrex-glass were made. For platinum electrodes, a lift-off process was used. Thermal oxide (500 nm thick) was grown on 4-inch silicon wafers. Evaporated hexamethyldisilazane (HMDS) served as an adhesion pro-

motor for the subsequent resist layer. Lithography was done by contact printing in standard optical resist. In the opened resist areas, oxide was etched 150 nm deep using an anisotropic reactive ion etching (RIE) process. The wafers were dipped in buffered HF-solution to obtain an undercut at the resist edges. Titanium (20 nm thick) serving as an adhesion layer and platinum (up to 150 nm thick) for the electrode and connector material were evaporated. The lift-off process was carried out in dimethylformamide (DMF) solution under sonication. Areas which acted as working electrodes could be encapsulated by a plasma-enhanced chemical vapour-deposited silicon nitride (PECVD-SiN_x:H) or silicon oxynitride (PECVD-SiON) layer (400 nm thick).

For the gold electrodes an electroplating process was used. A thermal oxide layer (500 nm thick) was grown on 4-inch silicon wafers. Pyrex-glass was directly used after a cleaning step. The substrate was covered with sputtered silicon nitride and a gold plating base. The lithography was performed by contact printing with a standard resist process for electrodes of up to 900 nm thickness. For submicrometre electrodes, e-beam lithography was used. In this case, 300 nm polymethyl methacrylate (PMMA 600 000) was spin coated. A prebake was performed for 30 min at 160 °C in a convection oven. The e-beam writing dose varied between 350 and 500 μC/cm² depending on the line and space dimensions [25]. The immersion development was done in methyl isobutyl ketone:isopropanol (MIBK:IPA, 1:2) for 90 s. A 30 min post-bake at 100 °C completed the resist process. Trenches were filled with 200 nm thick gold by pulse plating using a sulfidic plating solution [26]. Subsequently, the resist was dissolved in an acetone bath. The plating base was removed with an ion-milling step. Optionally, the electrode areas could be encapsulated with a 300 nm thick layer of sputtered silicon nitride.

The silicon and Pyrex wafers were sawn into single chips (9 mm × 9 mm), and the chips cleaned in DMF or acetone under sonication.

The chips were mounted in a standard semiconductor leadless ceramic carrier (JEDEC B Type, 68 Leads, Kyocera Fin ceramics, Japan) and connected by gold wire bonding. Gold bonding wires as well as extensive side feed lines of the electrodes were sealed and covered with 2-component glue (Epo-tek 302-3, Waldbronn, Germany), which has been found to show very low water absorption (see also Fig. 11a). Prior to cell inoculation, the chips were cleaned with one drop of 30% (w/w) hydrogen peroxide and three drops of concentrated H₂SO₄ for 3 min in an ultrasonic bath. They were then rinsed ten times with distilled water and sterilized for 20 min at 121 °C. Alternatively, the mounted chips were rinsed several times with distilled water, washed twice with 70% ethanol and subsequently sterilized at 110 °C for 3 h.

2.1.2. Microperforated silicon membranes

The process for microperforated silicon membranes started with an epitaxial grown layer with a phosphorous concentration of 10¹⁶ atoms/cm³. Thicknesses

of 3 μm and 5 μm were made. Both sides of the wafer were coated with thermal oxide (300 nm thick) followed by a low-pressure chemical vapour deposited silicon nitride (LPCVD-Si₃N₄) layer (140 nm thick). Silicon nitride was removed from the front, then optical lithography was performed to define the holes (first exposure) and the electrode structures (second exposure). The electrodes were produced as described under "microelectrode arrays". A third lithography step was used to define the rear cavities shown in Fig. 1. These cavities were anisotropically etched with 30% KOH at 80 °C using a pn-etch stop technique. A nitride protection layer was sputtered on the back of the membrane, then the epitaxial layer was opened from the front with 30% KOH at 80 °C. The nitride layer was subsequently removed.

Membranes of thickness 3 μm were chosen for use, one structure being shown in Fig. 1. There are three types of perforated fields with square pores whose edge length is 5 μm , 10 μm and 20 μm at the front surface of the membrane. The corresponding lengths are 1.25 μm , 6.25 μm and 16.25 μm at the back. The smaller pore dimensions at the back are a consequence of the manufacturing process (anisotropic etching). They may vary by a few micrometres, depending on the exact membrane thickness. The bridges between the pores at the front were 11.25 μm , 6.25 μm and 16.25 μm wide, respectively. The arrangement of electrodes on the bridges is shown in Fig. 10a for a field with large pores.

The microperforated chips were cleaned by heating in 70% ethanol, rinsed ten times with distilled water and sterilized as described above.

2.2. Origin and maintenance of cell lines

Swiss mouse embryo fibroblasts (NIH 3T3) were obtained from "Deutsche Sammlung von Mikroorganismen und Zellkulturen" (DSMZ, Braunschweig, Germany). Mouse fibroblast cell line L929 was a generous gift from Dr U. Zimmermann (University Würzburg, Germany). The L929 cell line was cultured in RPMI 1640 Medium with 5% foetal calf serum (FCS) and the 3T3 cell line in Dulbecco's modified Eagles Medium

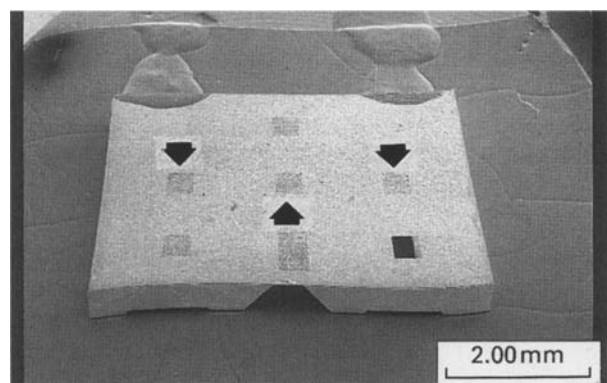


Figure 1 Structure of the microperforated silicon chip (SEM). View of a microchannel opening and a chip surface overgrown with fibroblasts (white dots). The small squares marked by an arrow are the perforated areas of the silicon membrane.

(DMEM) with 10% FCS at 37 °C in a humidified incubator gassed with 5% CO₂ in air. The confluent cells were split twice a week using 0.05/0.02% trypsin/ethylenediaminetetraacetic acid at 37 °C for 3–5 min. To remove the enzyme, the cells were subjected to 2–3 washing cycles with culture medium. Harvested cells were counted in a THOMA counting chamber and seeded into fresh medium at 1 × 10⁴ cells/ml.

2.3. Cell cultivation on microstructures

Experiments were carried out with cells cultivated for one day in a subculture. Harvested cells from the subculture were diluted with the culture medium to a final concentration in the range 2.5 × 10⁴ to 2 × 10⁵ cells/ml and seeded into Corning Disposable Multiple Well Plates (24 wells, 2 ml/well) containing the cleaned microstructures. The microstructures had been rinsed with phosphate buffered saline (PBS) without Ca²⁺ and Mg²⁺ and in some cases chips were coated with poly-L-lysine (Biochrom, Berlin, Germany) by incubating them with 0.5 ml solution (0.1 mg/ml) at 37 °C for 20 min.

2.4. Field application during cell cultivation

In these experiments special equipment (Fig. 2) was used, which allowed for the sterile incubation of the microstructures mounted and bonded in the ceramic carriers. The culture chamber containing the microstructure was sterilized as described for the microelectrode arrays. 1–4 × 10⁵ cells were seeded in 1.5 ml of medium in the chamber which was then incubated at 37 °C in humidified air containing 5% carbon dioxide. Electric fields were applied using a rectangular pulse generator (pulse/function-generator 50 MHz, 8116A, Hewlett Packard, US). The output waveform at the electrode chamber was monitored by a digitizing oscilloscope (54503A, 500 MHz, Hewlett Packard, US). The application of high frequency a.c. fields to the incubator started 2–4 min after inoculation and was extended over a period of up to 30 h. Symmetrical a.c. fields with a frequency of 5 MHz (duty cycle 50%) and a voltage range from 1.5 to 3.5 V peak-to-peak were used.

2.5. Light microscopy

Cells were monitored in the culture medium or PBS and after fixation in 3.9% formalin and staining with Giemsa azure-eosin-methylene-blue (Merck, Darmstadt, Germany) using a Leitz Metallux (Leica, Wetzlar, Germany) designed for reflected light microscopy and a Leitz Aristoplan (Leica, Wetzlar, Germany) with differential interference contrast. Images were recorded on Fujicolor 200 colour negative film.

2.6. Scanning electron microscopy (SEM)

Cells adherently grown on silicon and glass chips were washed three times with warmed PBS and fixed with 2.5% (v/v) glutaraldehyde in PBS at 4 °C for 30 min. Glutaraldehyde was diluted from a 25% stock solution immediately before fixation. The specimens were

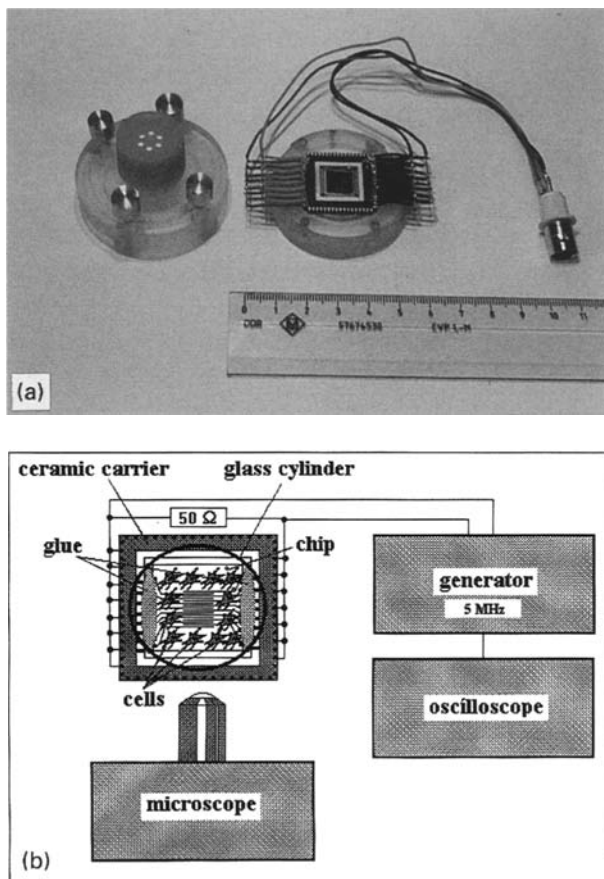


Figure 2 Device for cell cultivation under electric field: (a) cultivation chamber; (b) experimental setup. Microstructures were mounted and bonded in a ceramic carrier. Electrical connections were made with short cables soldered to the gold connections of the carrier and terminated with a BNC plug. A removable glass cylinder (22 mm in diameter and 11 mm high) coated with silicone (0.2–0.5 mm thickness) at the ends was fixed on the carrier by means of two Perspex elements clamped with four screws. An opening in the top enabled inoculation with cells, microscopic observation and changes of solutions (medium, dye). This was closed with the gas permeable cover of a cell culture flask. A 50 cm BNC cable (the short total cable length is necessary to avoid reflections) connected the culture chamber to the pulse generator. The oscilloscope was used to monitor the output waveform at the electrode chamber, and the microscope to follow cell growth.

then well rinsed with PBS, postfixated with OsO_4 (2%, w/v) in PBS for 10 min at room temperature and further washed with PBS (once) and double distilled water (twice). The specimens were immersed in 30% (v/v) ethanol, transferred through a concentration series of ethanol (40, 50, 60, 70, 80, 90, 96%) and finally brought into absolute ethanol or acetone. The organic solvent was removed by critical point drying with CO_2 (CPD 030, Balzers Union Company, Liechtenstein) or, in some cases, by simply drying in air.

The dried specimens were mounted onto an aluminium specimen holder covered with conducting adhesive tape. To increase the conductivity a “bridge” of conducting carbon was deposited between the chip and the holder. Finally the surface of the specimen was sputter-coated with platinum for 5 min at 30 mA (SCD 050, Balzers Union Company, Liechtenstein). The specimens were examined at an accelerating voltage of 15–20 kV using a Leica S 360 scanning electron microscope. Images were recorded on Polaroid 4 × 5 instant sheet film, Type 53.

3. Results

3.1. Growth of fibroblasts on conventional substrates

Fibroblasts of 3T3 and L929 cell lines used in our experiments showed the well known phenomena of anchorage, flattening and moving on plastic (well plates) and glass (cover glasses) surfaces. At the beginning of subculture, after trypsination the cells were of spherical shape with a diameter of about 15 μm . After inoculation they sedimented onto the substrate surface and anchored there. These processes were complete after 25 min (3T3) or 45 min (L929).

After anchoring, the cells began to flatten and to spread. During this process the cell borders became less visible with simple transmitted light microscopy but could be observed with Nomarski interference contrast (Figs 3a, 4a). Giemsa staining after formalin fixation as well as vital staining with fluorescein-diacetate (FDA) produced highly contrasted images but could be applied only if permanent maintenance of cell vitality was not necessary.

Cells appeared to be well adherent. They were not washed away by shear forces during medium exchange or rinsing with PBS before microscopy. However, after reaching confluence, the whole cell layer (especially 3T3 cells) might detach from untreated cover glasses during these procedures. This could be prevented by coating the glass with polylysine.

3.2. Growth of fibroblasts on microchips

The fibroblasts were able to grow on microstructured silicon and glass substrates if chips were cleaned as described in the methods section. The adherence of the cells could be improved by coating the chips with polylysine (important for 3T3 cells after reaching confluence). Different microstructures with typical electrode dimensions in the micrometre and sub-micrometre range were tested successfully. In all cases normal anchorage and spreading of the cells was observed. Differences in cell density resulted only from the inoculation.

In Figs 3 and 4 some examples with simple arrays of gold and titanium/platinum electrodes on glass and silicon chips are presented. The figures show that the cells are distributed more or less uniformly over the whole chip surface and did not prefer one or other of the surface materials. Similar results were obtained with more sophisticated microstructures, where electrodes were made from Ti/Pt and partly covered with a thermally sputtered silicon oxynitride (Fig. 3d).

In the experiments presented here only electrodes less than 1 μm in height were used. They did not act as growth obstacles to the tested cells. Scanning electron microscope (SEM) images (Fig. 4c, d) show that the cells were able to cross the boundary between the chip surface and the electrode, presumable in both directions. Therefore, they have to cross two right angles, one external and one internal. Disruptions of cell filopodia as well as fissures in the cell body are artefacts caused by shrinking during dehydration or by critical point drying of the specimen.

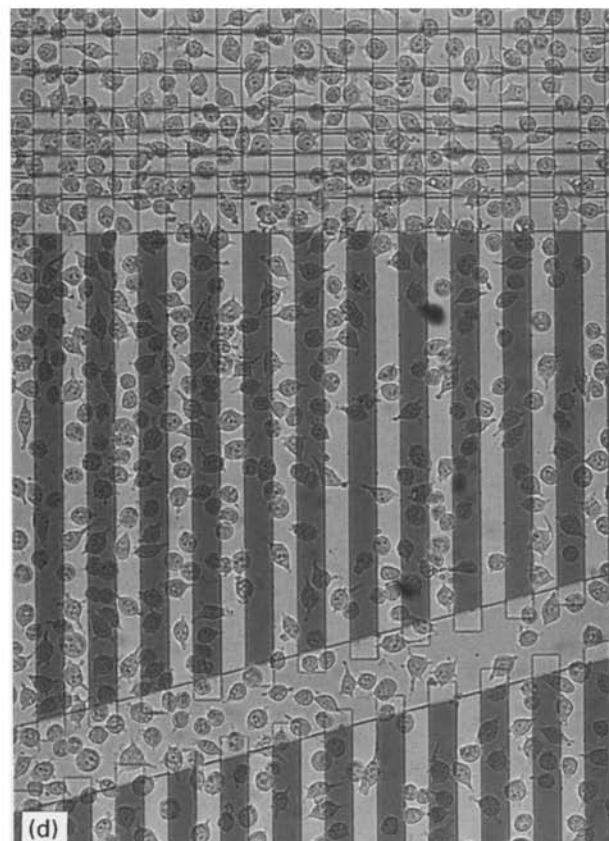
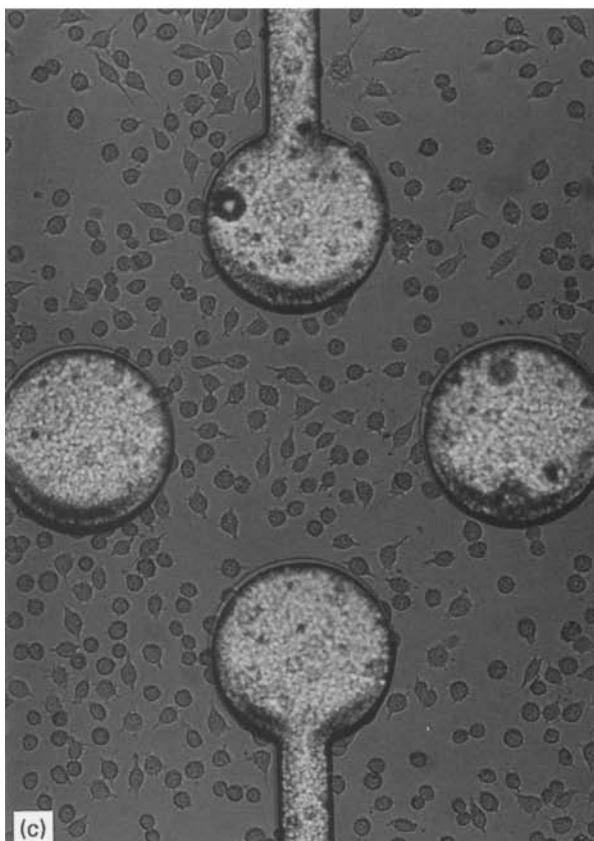
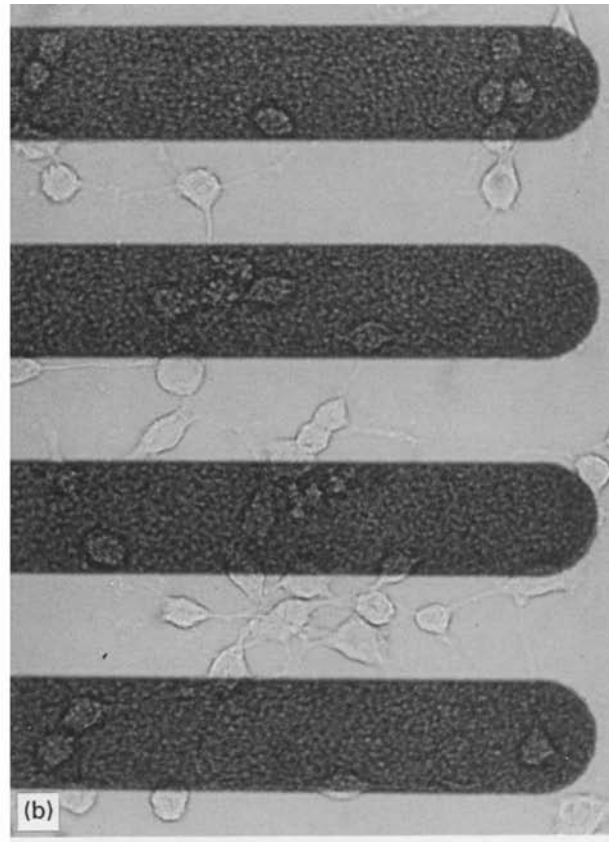
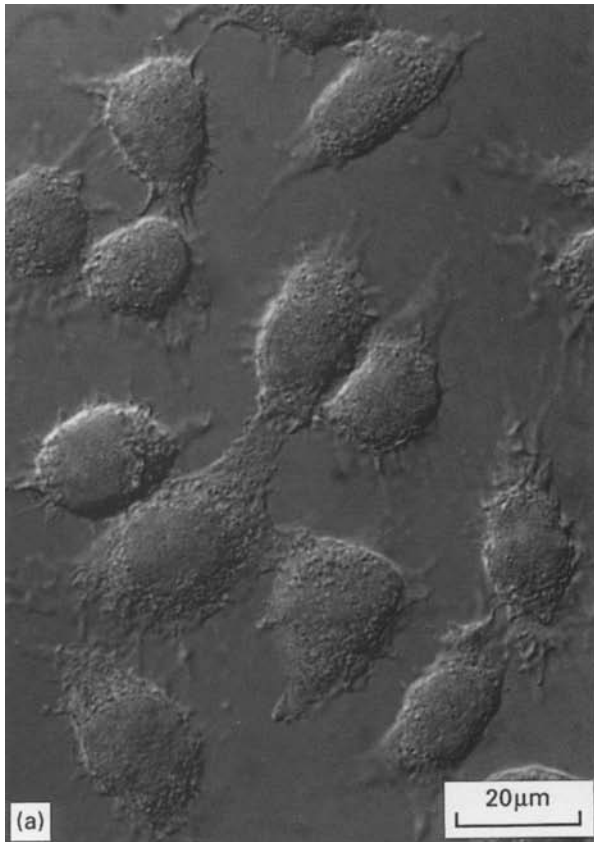


Figure 3 L929 cells grown on glass and silicon surfaces covered with metal electrodes: (a) glass chip, differential interference contrast; (b) glass chip with gold electrodes (950 nm height, 50 μm width), transmitted/reflected light; (c) silicon chip with 950 nm high gold electrodes, distance between the opposite electrodes was 200 μm , reflected light; (d) silicon chip with Ti/Pt (25 nm/150 nm height, 30 μm width) electrodes partly sputtered with silicon oxynitride (400 nm PECVD-SiON). The structures in b, c and d can be used for single-cell manipulation, cultivation and characterization by electrorotation (see [25]).

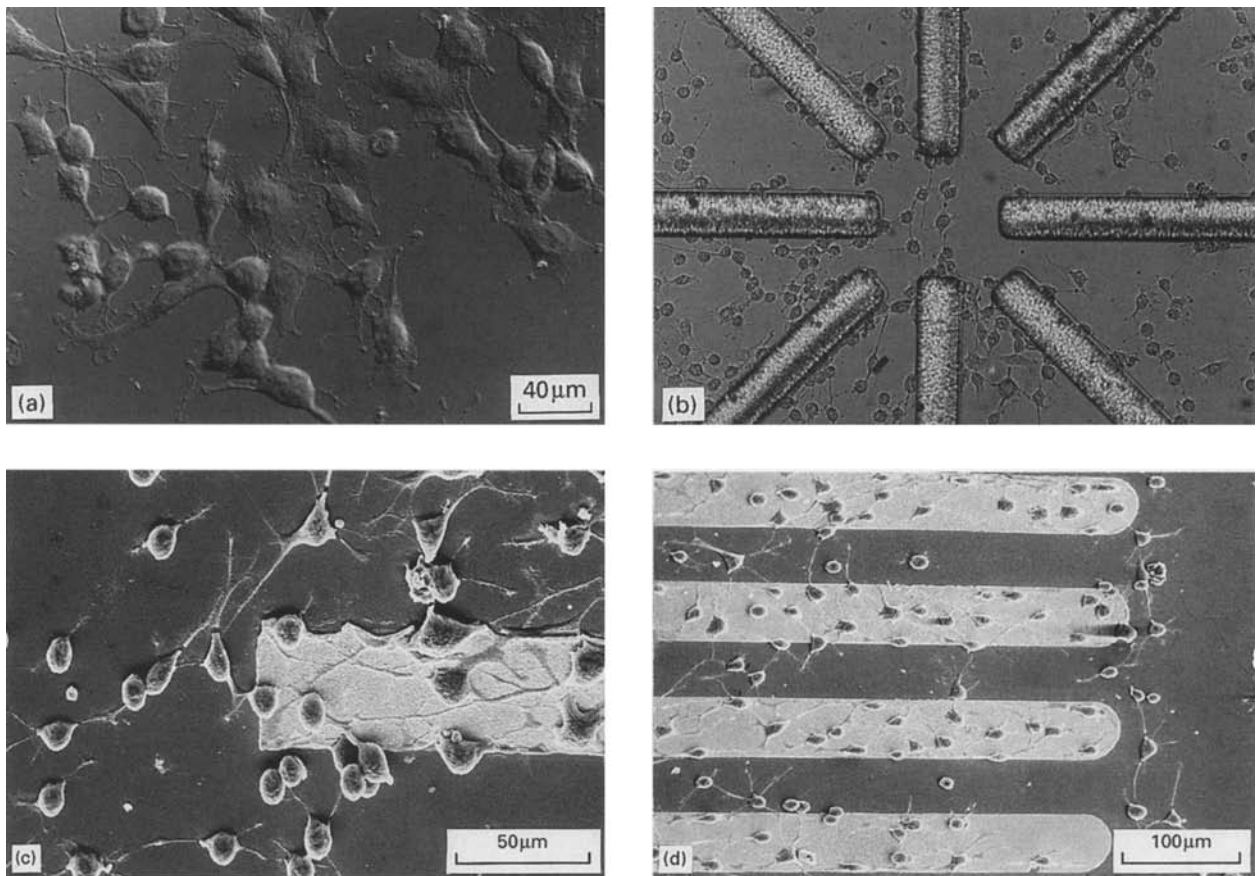


Figure 4 3T3 cells grown on glass and silicon surfaces structured with gold electrodes: (a) glass chip, differential interference contrast; (b) silicon chip with gold electrodes (950 nm height, 75 μm width), reflected light; (c, d) glass chips with gold electrodes (950 nm height, 50 μm width) (SEM).

3.3. Growth of fibroblasts on microperforated membranes

Fibroblasts of the cell lines 3T3 and L929 were cultivated on silicon chips containing pore fields with square holes of different size (5 \times 5 μm , 10 \times 10 μm , 20 \times 20 μm). The overall thickness of the wafers was 500 μm but in the area of the pore fields they formed a perforated membrane of only 3 μm . This membrane is translucent and therefore cells on it can be observed by transmitted light microscopy.

Cells of both cultures were able to grow on the perforated membranes. If the cells were seeded at sufficient density (about 10^5 cells/ml), they formed a confluent layer on the whole chip including the pore fields after about 20 h (Figs 7b, 8a). In this paper, we mainly report the behaviour of L929 cells on perforated membranes; the 3T3 cells showed very similar behaviour but adhered less strongly to the membrane surface (see above).

The cell distribution on the pore fields was studied by SEM. Cell density has been chosen so that cells covered all the chip surface but did not reach complete confluence. This allowed better distinction of the cell boundaries. In the case of small pores (5 μm \times 5 μm) the lengths and shapes of the cells growing on the pore fields did not differ from those growing on smooth glass and silicon chips. This is clearly demonstrated in Fig. 5a. Here the boundary between the perforated membrane (left side) and the surrounding unper-

forated area (right side) is shown. On both surfaces cells were distributed uniformly; some cells are located directly on the boundary. It seems clear that small pores did not disturb attachment and spreading of the cells. The cells were able to spread over the pores and to cover them completely, in some cases more than one pore (Fig. 5b). With pores of 10 μm \times 10 μm (Fig. 5c, d) cell spreading mainly occurred on the bridges between the pores, but cells inserted their filopodia into the pores and sometimes more or less filled them. The 20 μm \times 20 μm pores were larger than the cells. Cells were found mainly on the relatively wide bridges between the pores where they were able to spread (Fig. 6a, b). The cells also sent filopodia into the pores. Some cells were localized in pores, did not spread within them and kept their spherical shape (Fig. 6c). Occasionally cells were found which partially covered a pore (Fig. 6d). The coverage remained incomplete although on the unperforated surface a single cell could cover an area greater than 1000 μm^2 . However, with 20 μm \times 20 μm pores complete coverage of the pore fields occurred if high cell densities were reached and cells began to form a multi-layer.

When the cell layer was gently removed from the front surface of the silicon membrane, it could be seen that cells had also reached the back (Fig. 7a). These were localized mainly below the pore fields and extending radially from them. The cells near a pore field

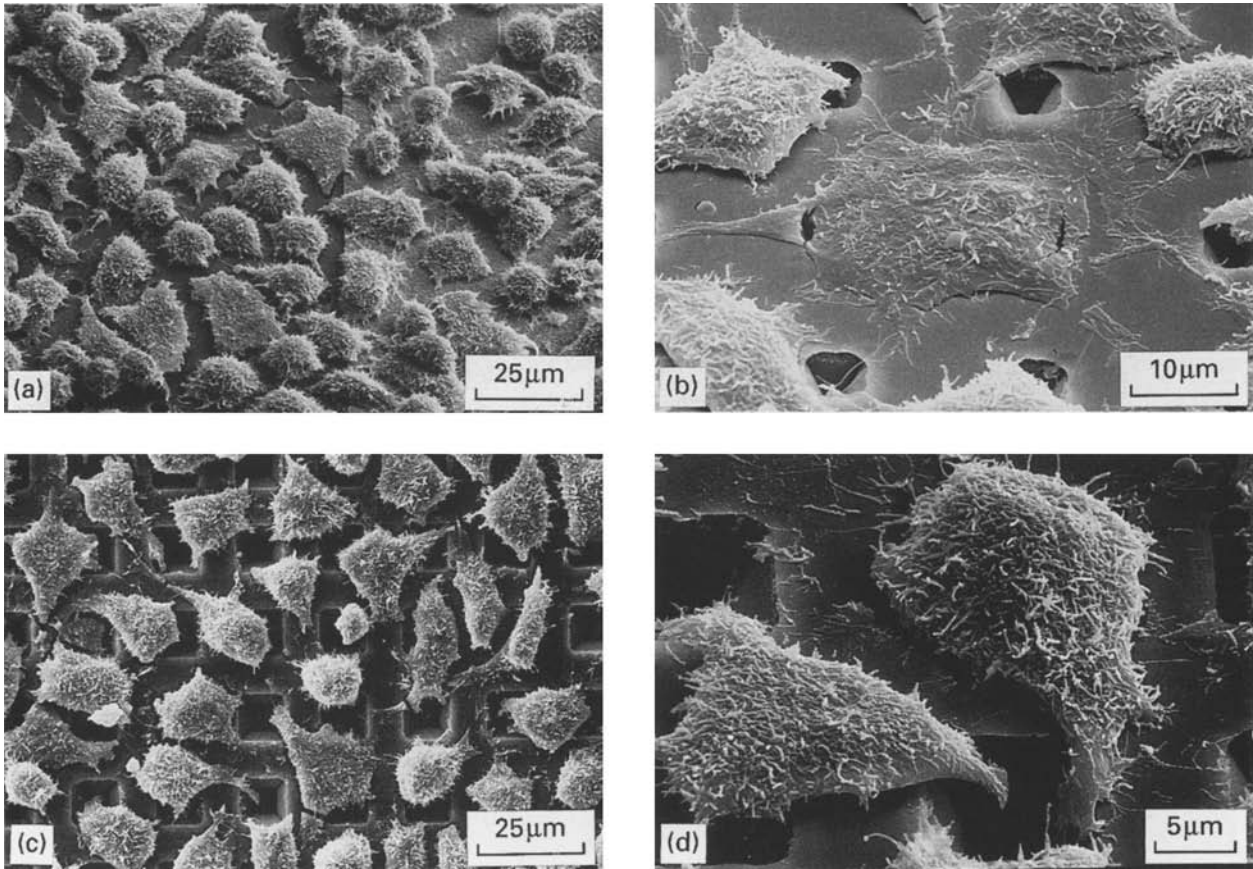


Figure 5 The covering of pores by fibroblasts (L929) grown on microperforated silicon membranes of 3 µm thickness (SEM); pore size: (a, b) 5 × 5 µm and (c, d) 10 × 10 µm (for details see text).

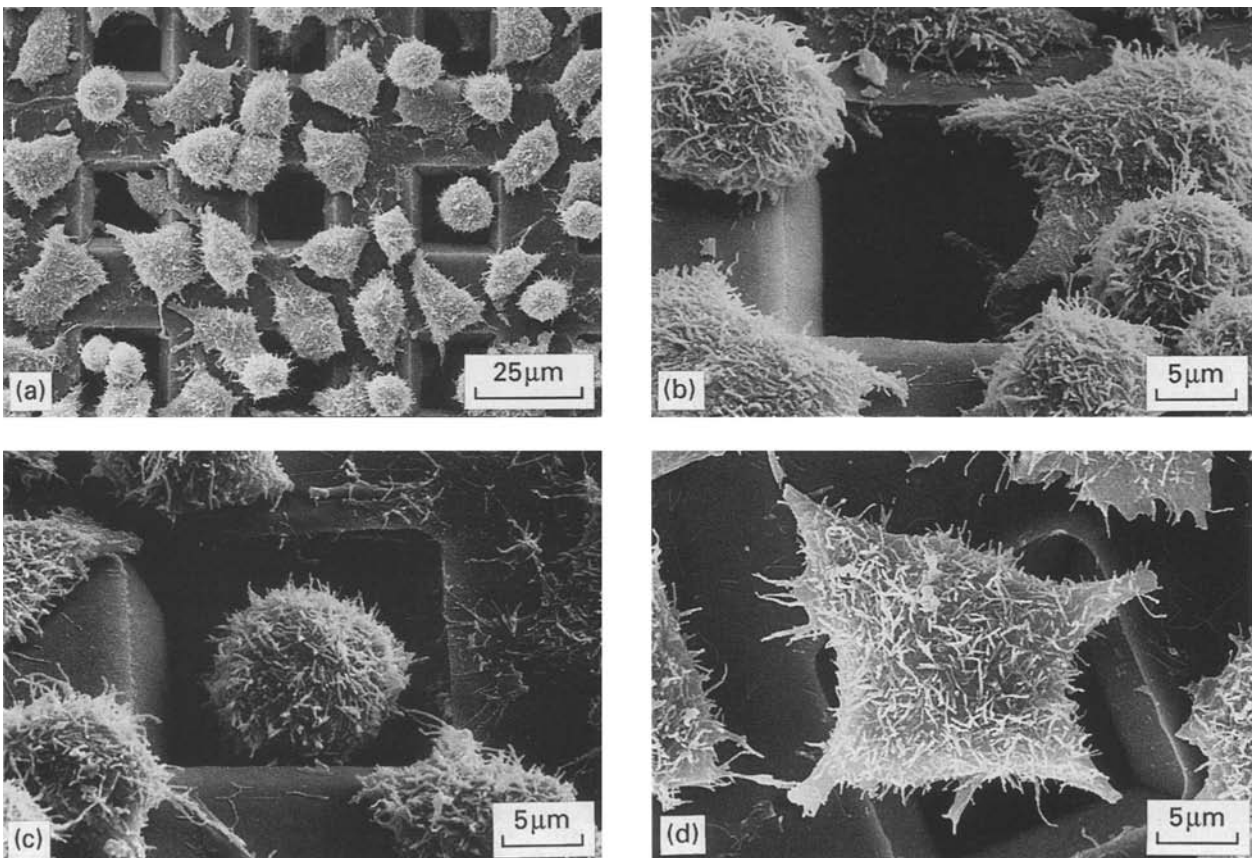


Figure 6 Fibroblasts (L929) surrounding, occupying or incompletely covering 20 × 20 µm pores in a silicon membrane of 3 µm thickness (SEM).

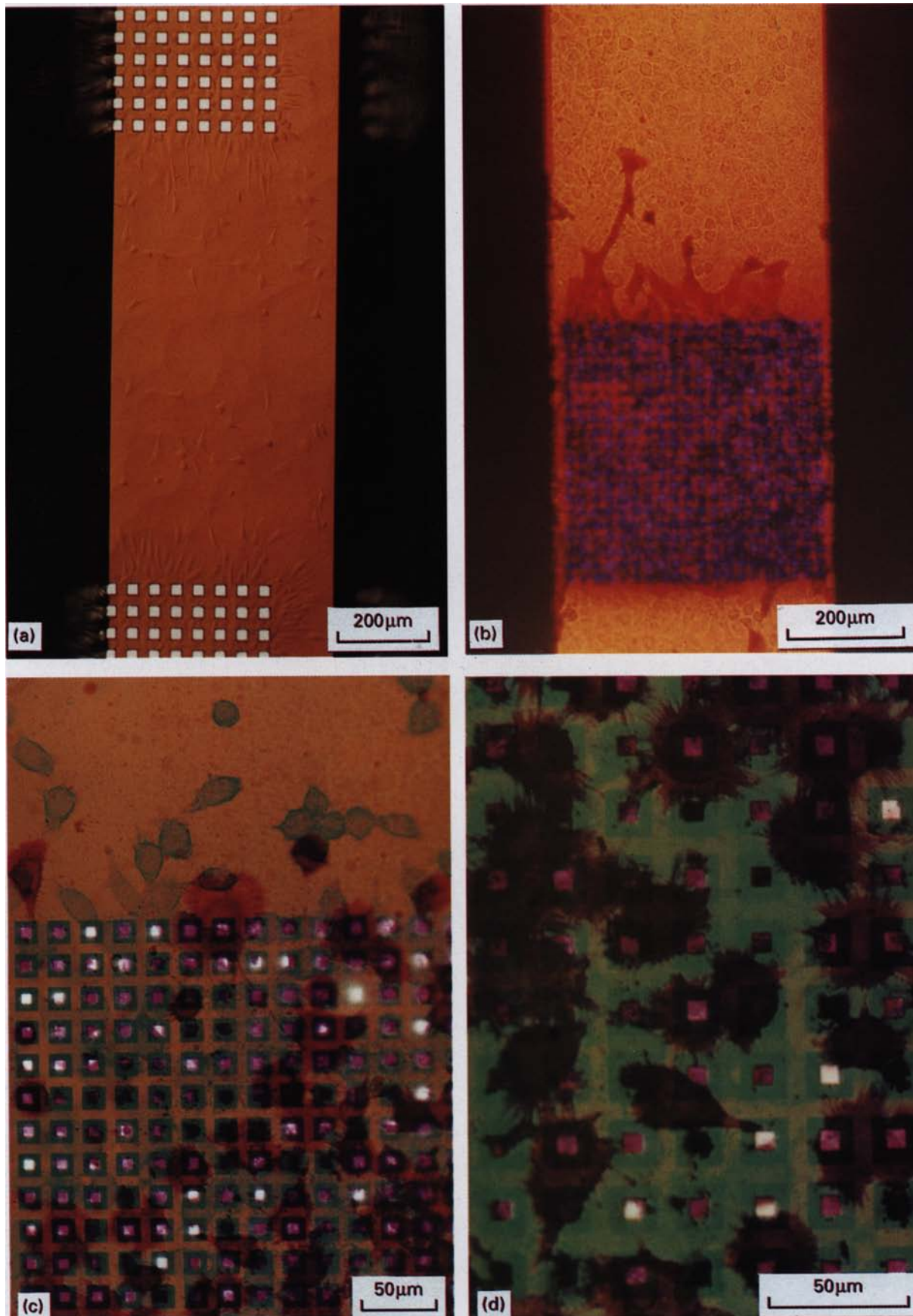


Figure 7 Distribution of fibroblasts on both sides of a perforated silicon membrane seen from the bottom. (a) L929, transmitted light, pore size $20 \times 20 \mu\text{m}$; cells on the top surface have been removed, only the cells on the bottom side remain. (b–d) In order to visualize cells simultaneously at both sides of the membrane (pore size $10 \times 10 \mu\text{m}$) they were overstained with Giemsa dye solution. The cells behind the membrane appear less stained and so could be distinguished clearly from the others using transmitted (b, 3T3) or a combination of transmitted and reflected light illumination (c, d, L929).

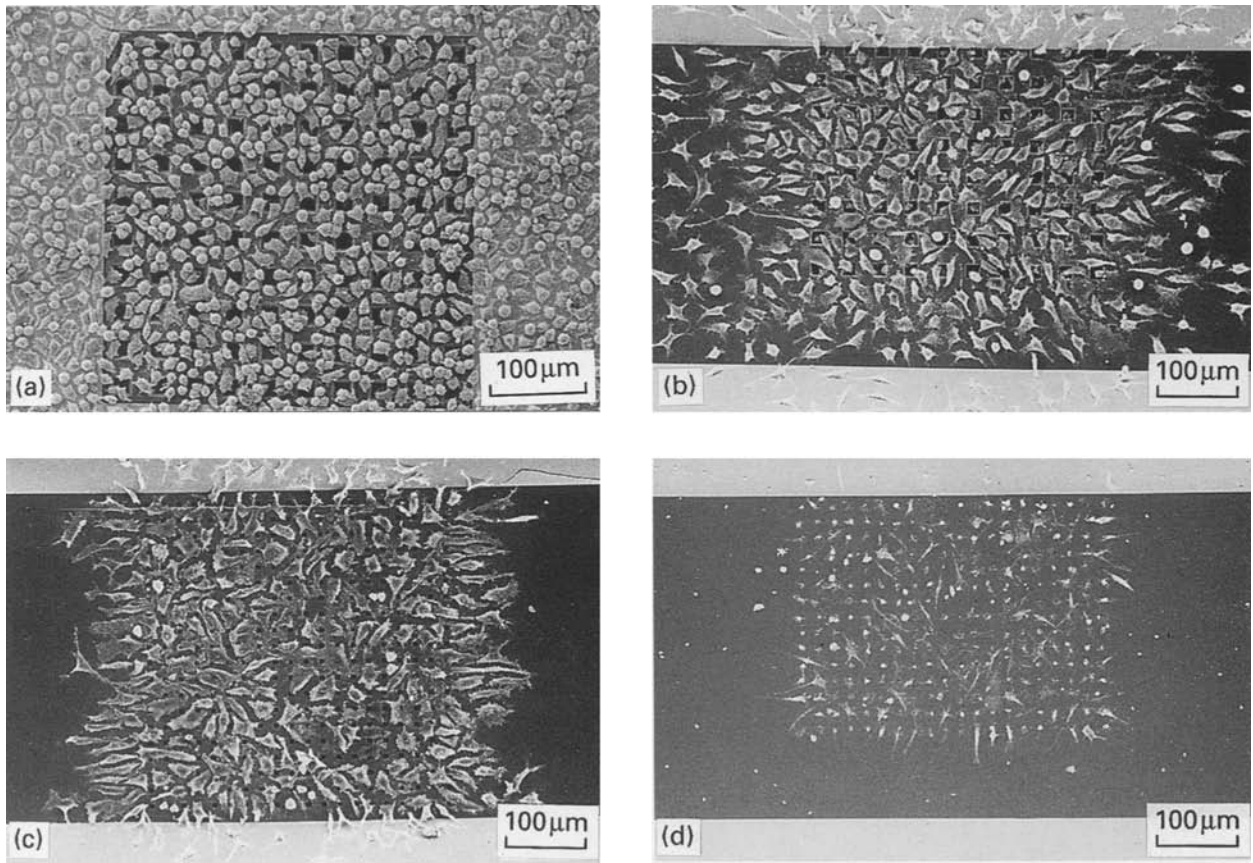


Figure 8 SEM-view of the distribution pattern of fibroblasts (L929) grown on microperforated silicon membranes in comparison to Fig. 7: (a) top of the membrane, $20 \times 20 \mu\text{m}$ pores; (b-d) bottom of the membrane, pore size: 16.2×16.2 , 6.2×6.2 , $1.2 \times 1.2 \mu\text{m}$ corresponding to 20×20 , 10×10 , $5 \times 5 \mu\text{m}$ at the top.

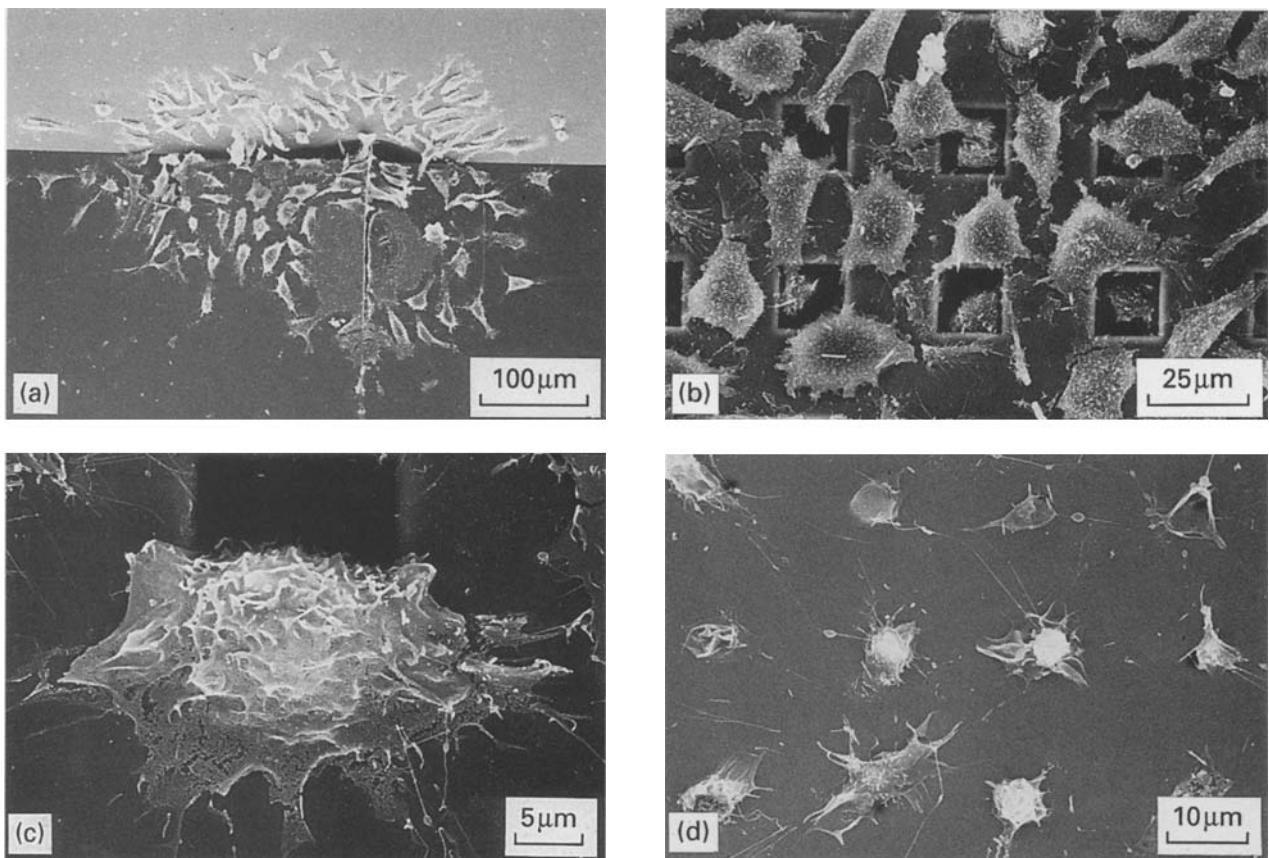


Figure 9 Detailed view of the localization and shape of fibroblasts at the bottom of a silicon membrane after and during crossing through pores or fissures. (a) Cells surrounding a membrane fissure; (b) cells spread at the bottom side of a field with $20 \times 20 \mu\text{m}$ pores; some cells had not left the pores; (c) single cell crossing a $20 \times 20 \mu\text{m}$ pore; (d) cells localized in/below $5 \times 5 \mu\text{m}$ pores.

were of long narrow shape and roughly perpendicular to the field boundaries. There were a few non-oriented cells below the unperforated membrane area between pore fields. The number of cells below the pore fields depended on the pore size at the rear of the membrane. After 24 h incubations, many cells were found below the large and medium pores but only a few, very small cells (possibly only a part of the whole cell body) below the small ones (Fig. 8).

We tested the hypothesis that cells were able to crawl through the pores to the back of the membrane. We attached a glass cylinder to the chip so that it surrounded one or two medium-sized pore fields. The open end of the cylinder stood out above the cell-free medium in which the chip was immersed. Cells were introduced only into the cylinder. There was no possibility that cells could reach the rear of the membrane by convectional streaming in the bulk medium. After an incubation time of 24 h cell distribution on both sides of the chips was observed (Fig. 7b–d). Cells were found above and below the membrane but only in that area which was bounded by the cylinder. They showed the same distribution pattern as in the former experiments. On the upper side of the membrane, cells were distributed uniformly. On the underside, they were located mainly below the pore fields as shown in

Fig. 8. In some cases thin fissures (several micrometres in width) appeared in the silicon membrane during preparation. Cells were found also around such fissures (Fig. 9a).

In order to visualize cells on both sides of the membrane at the same time, contrast was enhanced by Giemsa staining after formalin fixation (Fig. 7b–d). Chips were examined from the underside with transmitted light (Fig. 7b) or using a combination of transmitted and reflected light (Fig. 7c, d). Cells located behind the membrane, i.e. on the upper side, appear less intensely stained. Fig. 7c shows that cells appeared below the pore fields before those on the upper side of the membrane reached confluence. The silicon membrane pores do not show uniform staining. Those which appear stained are covered by cells on one or both sides, whereas the white ones are uncovered.

SEM gives a more detailed picture of cells crossing pores (Figs 8, 9). Fig. 9b shows cells which had crossed the large pores from the top, anchored and spread on the bridges between pores. Some cells are still localized within the pores. Fig. 9c shows a cell just leaving one of the large pores. Similar pictures could be obtained below the medium pores. Small pores (usually $1.2\ \mu\text{m} \times 1.2\ \mu\text{m}$, but $0.8\ \mu\text{m} \times 0.8\ \mu\text{m}$ here) slowed down cell crossing. After 24 h, cells were still restricted

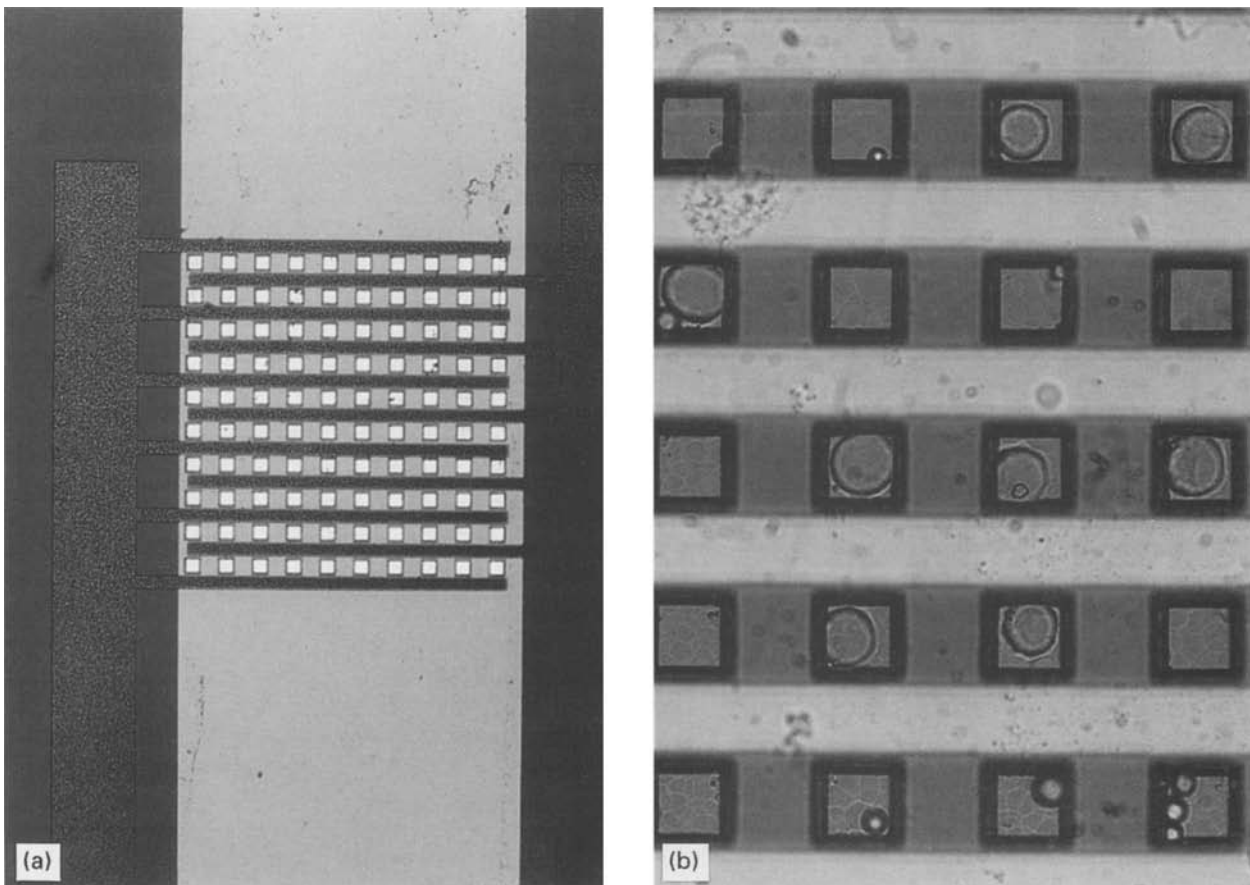


Figure 10 Selective positioning of cells on a microperforated membrane by negative dielectrophoresis caused by a high frequency electric field (a.c. square wave, 5 MHz, 0.6 V p to p) applied to thin electrodes on the narrow bridges between the holes. The pore size (within the heavy black border) is $16.2 \times 16.2\ \mu\text{m}$. (a) Overview of the electrode arrangement; (b) fibroblasts (3T3) deposited in the pores. Suspended cells were forced to the pores between the electrodes and allowed to anchor. Those cells which did not anchor were washed away. (In order to avoid cell crossing through these pores the pores were closed at the bottom by an Epo-tek layer. Small latex particles (3–10 μm , Standard Dow Latex, SERVA, Heidelberg, Germany) can also be moved to the pores by negative dielectrophoresis. Sometimes they could not be washed away due to their small size in comparison with pore dimensions.)

to a relatively small area around the single pores (Fig. 9d), although at the top side of the membrane the cell layer was already confluent. The cells below the membrane differ markedly from the others in size and shape (compare also Fig. 8) as well as being fewer in number. Probably, a part of the cell body remained at the other side of the silicon membrane. In most of these cells a nucleus was found by fluorescence detection after staining with propidium iodide (images not shown).

3.4. Prevention of cell anchoring by means of high frequency electric fields

To deposit cells accurately over holes we developed a structure combining microperforated square pores with interdigitated electrodes as shown in Fig. 10a. The pores and electrodes are of similar dimensions to the cells (edge length 20 μm ; electrode width and gap 20 μm ; cell diameter 16 μm). With no field applied, the cells distributed uniformly over the whole chip surface. High frequency a.c. fields repel cells into the interelectrode space. Field strength in the holes is lower than in the regions between them, consequently, cells collect preferentially in the square pores (see

Fig. 10b). Unfortunately, during prolonged cultivation under applied field, adherently growing cells could cross the electrodes and field gradients by active motion. Electrode geometry in this preliminary structure is not yet optimized. It may be possible to overcome this problem by using interdigitated arrays of micrometre or submicrometre electrodes to increase the gradients.

Ultra-microelectrode-arrays, consisting of 32 individually addressable, interdigitated linear electrodes were used in preliminary experiments (Fig. 11a; electrode space and width each 0.2 to 3 μm in central area). The electrodes were as small as possible to achieve high field strength near the surface and to increase the negative dielectrophoretic effect. The electric field spreads no further than a few interelectrode gaps from the surface. Cells entering this region are repelled, cannot approach the surface and therefore cannot attach. Initially cell adhesion did not occur in the central (high field) part of the array. Fig. 11b shows the device after 48 h of cultivation of mouse 3T3 fibroblasts under high frequency field. During this time cells had gradually occupied the interdigitated electrode array parallel to the electrodes and the

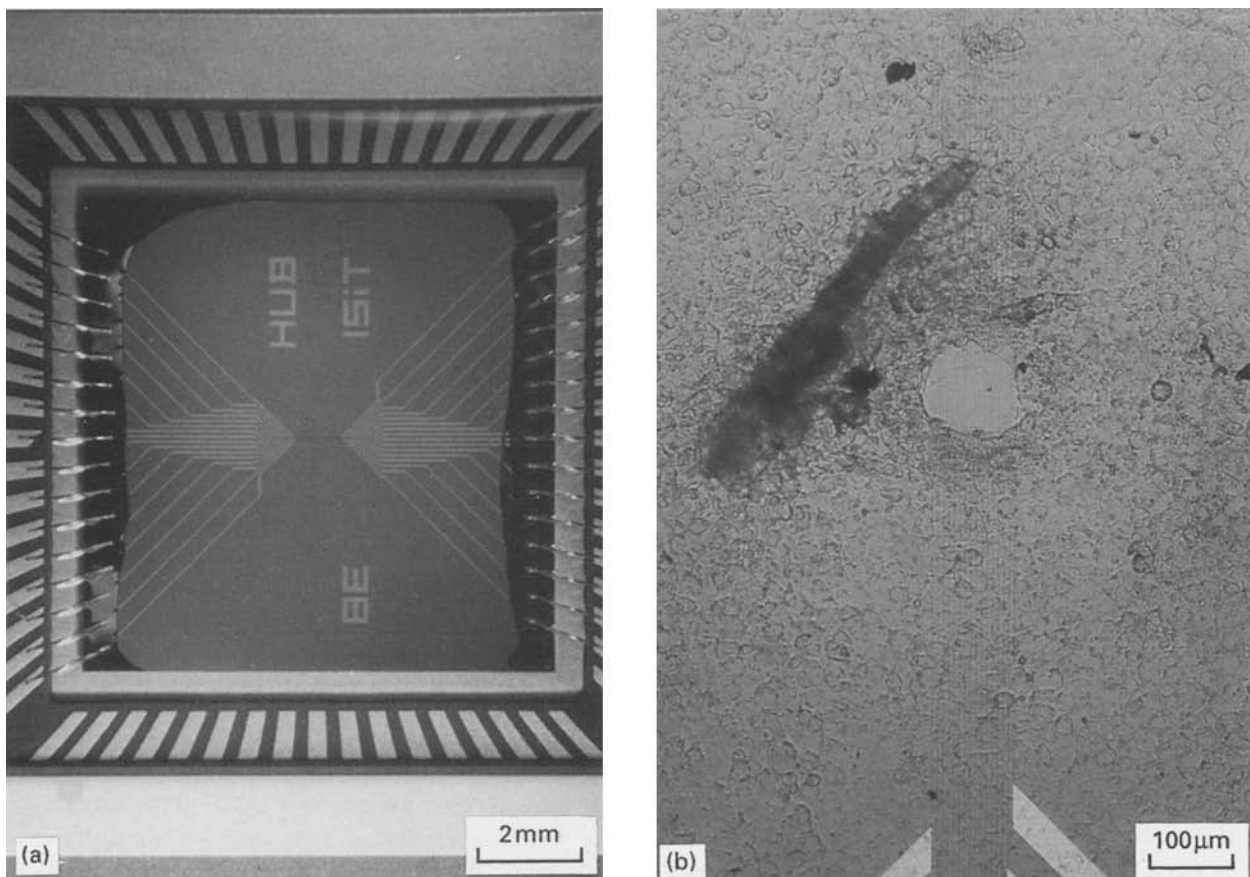


Figure 11 Prevention of cell anchoring by high frequency electric fields. (a) Ultramicroelectrode array, consisting of 32 individually addressable, interdigitated linear electrodes (gold, height 900 nm, electrode width 1 μm and space 2 μm in central area of 200 \times 100 μm). The chip was mounted and bonded in the ceramic carriers. Gold bonding wires as well as extensive side feed lines of the electrodes were sealed and covered with two-component glue. (b) The same microelectrode structure after 48 h cultivation of 3T3 fibroblasts (inoculated with 8×10^4 cells/ml in 1.5 ml, correspond to a cell density of 423 cells/ mm^2) under permanent field (a.c. square wave, 2 V p to p, 5 MHz). The whole chip surface was covered by a confluent layer of vital cells. An area of 124 \times 100 μm of the interdigitated electrodes (200 \times 100 μm) remained completely free of cells. During culture cells gradually occupied the electrode array parallel to the electrodes and the interelectrode gaps up to a depth of 38 μm . Directly around the cell free-electrode region the fibroblasts were multi-layered.

interelectrode gaps up to a depth of 38 μm , but an area of 124 \times 100 μm remained completely free of cells.

4. Conclusions

The questions developed in the introduction can now be answered.

Fibroblasts grow without marked changes in behaviour on microstructured glass or silicon surfaces, even under prolonged field application. Strong high frequency electric fields can be used to repel cells from surfaces by negative dielectrophoresis. Active adhesion control of areas in the square micrometre or square millimetre range can be achieved (see also [28]). Surface topography, such as walls, edges or holes, influences the motility and spreading of cells and can be used to control the direction and localization of cell growth (see review [9]). Silicon membranes perforated by square pores are well suited for the study of fibroblast motility near edges. We have to distinguish between two kinds of fibroblast growth: (i) covering the pores and (ii) crossing the pores. Both types of growth are important for characterization of single cells by impedance or noise analysing techniques (see also [16, 18, 19]). For the fibroblasts used here, 5 \times 5 μm pores could be completely covered by a cell (Fig. 5a, b). It would be interesting to investigate the organization of the cytoskeleton in a cell spreading over a pore, especially in that part of the cell body which is not in contact with the surface of the substrate. 10 \times 10 μm holes were sometimes covered by cells and sometimes contained cells (Fig. 5c, d). At a pore size of 20 \times 20 μm cells adhered to the silicon bridges or moved into the pores (Fig. 6).

Cells could go through pores much smaller than typical cell dimensions. Pores larger than 6.2 μm \times 6.2 μm (bottom side of the 10 \times 10 μm pores) were freely crossed by fibroblasts. Most smaller pores (Fig. 9) are completely filled by one (only) fibroblast with parts of the cell anchored on both sides of the silicon membrane. Note that such an arrangement/fixing of single cells is very suitable for their passive electrical characterization (impedance, micropipette technique, current analysis, patch clamp).

The fibroblasts grew around an angle of more than 50 degrees from the top side of the silicon membrane into the pore and an angle of more than 120 degrees from the pore to the back of the chip. Obviously fibroblasts are able to do this although Dunn and Heath [29] claimed that motion over an angle of pitch greater than 16 degrees is impossible, probably due to the cytoskeleton in the leading lamellae. However, there is some evidence from other investigations [6, 30] that this behaviour of cells cannot be generalized.

Three-dimensional structuring of silicon and glass substrates opens up new possibilities for the development of single cell measuring and manipulation techniques. The accuracy of the etching technique is in the submicrometre range. Pores between several hundred nanometres and several hundred micrometres can be made. However, little is known about cell behaviour on such structured surfaces. A practical application of the ability of cells to traverse micropores might be

powerless separation devices [31]. Different cell types require different pore dimensions and geometries to cross thin silicon membranes. So they could be separated in counter current fluid microchannel systems. However, the production of accurate working microsystems requires a profound knowledge of cell behaviour. To contribute to this work was the aim of this paper.

Acknowledgements

We thank Dr M. Wenzel and Mrs H. Weise from Institut für Anatomie, Med. Fak. der HUB, Universitätsklinikum Charité (Berlin) for critical point drying and sputter coating of the specimen for SEM and Mrs U.-H. Hebermehl and Mr H. Saft for excellent technical assistance. This work was supported by the BMFT (grant no.: 13MV03032).

References

1. C. O'NEILL, P. JORDAN and G. IRELAND, *Cell* **44** (1986) 489.
2. C. O'NEILL, P. JORDAN, P. RIDDLE and G. IRELAND, *J. Cell Sci.* **95** (1990) 577.
3. P. CLARK, P. CONNOLLY and G. R. MOORES, *ibid.* **103** (1992) 287.
4. P. CLARK, ST. BRITLAND and P. CONNOLLY, *ibid.* **105** (1993) 203.
5. R. SINGHVI, A. KUMAR, G. P. LOPEZ, G. N. STEPHANOPOULOS, D. I. C. WANG, G. M. WHITESIDES and D. E. INGBER, *Science* **264** (1994) 696.
6. J. A. DOW, P. CLARK, P. CONNOLLY, A. S. G. CURTIS and C. D. W. WILKINSON, *J. Cell Sci. Suppl.* **8** (1987) 55.
7. P. CLARK, P. CONNOLLY, A. S. G. CURTIS, J. A. T. DOW and C. D. W. WILKINSON, *Develop.* **108** (1990) 635.
8. *Idem.*, *J. Cell Sci.* **99** (1991) 73.
9. A. S. G. CURTIS and P. CLARK, *Critic. Rev. Biocomp.* **5** (1990) 343.
10. Y. JIMBO, H. P. C. ROBINSON and A. KAWANA, *IEEE Transact. Biomed. Eng.* **40** (1993) 804.
11. K. F. WEIBEZAHN, G. KNEDLITSCHKE, H. DERTINGER, W. BIER, T. SCHALLER and K. SCHUBERT, *Bioforum* **17** (1994) 49.
12. P. FROMHERZ, A. OFFENHAUSSER, T. VETTER and J. WEIS, *Science* **252** (1991) 1290.
13. S. TATIC-LUCIC, Y.-C. TAI, J. A. WRIGHT, J. PINE and T. DENISON, in Proceedings 7th International Conference on Solid-State Sensors and Actuators, Transducers '93, Yokohama, Japan (1993) p. 943.
14. G. T. A. KOVACS, C. W. STORMENT, M. HALKS-MILLER, C. R. BELCZYNSKI, C. C. DELLA SANTINA, E. R. LEWIS and N. I. MALUF, *IEEE Transact. Biomed. Eng.* **41** (1994) 567.
15. I. GIAEVER and C. R. KEESE, *Proc. Natl. Acad. Sci.* **81** (1984) 3761.
16. R. LIND, P. CONNOLLY, C. D. W. WILKINSON, L. J. BRECKENRIDGE and J. A. T. DOW, *Biosens. Bioelectron.* **6** (1991) 359.
17. G. FUHR, W. M. ARNOLD, R. HAGEDORN, T. MÜLLER, W. BENNECKE, B. WAGNER and U. ZIMMERMANN, *Biochim. Biophys. Acta* **1108** (1992) 215.
18. I. GIAEVER and C. R. KEESE, *Proc. Natl. Acad. Sci.* **88** (1991) 7896.
19. CH.-M. LO. C. R. KEESE and I. GIAEVER, *Exp. Cell Res.* **204** (1993) 102.
20. J. Z. BAO, C. C. DAVIS and R. E. SCHMUKLER, *IEEE Trans. Biomed. Eng.* **40** (1993) 364.
21. TH. SCHNELLE, R. HAGEDORN, G. FUHR, S. FIEDLER and T. MÜLLER, *Biochim. Biophys. Acta* **1157** (1993) 127.

22. H. A. POHL, in "Dielectrophoresis" (Cambridge University Press, Cambridge, 1978).
23. R. PETHIG, Y. HUANG, X.-B. WANG and J. P. H. BURT, *J. Phys. D: Appl. Phys.* **24** (1992) 881.
24. W. SCHÜTT, H. KLINKMANN, I. LAMPRECHT and T. WILSON, "Physical characterization of biological cells" (Verlag Gesundheit GmbH, Berlin, 1991).
25. G. FUHR, H. GLASSER, T. MÜLLER and TH. SCHNELLE, *Biochim. Biophys. Acta* **1201** (1994) 353.
26. C. KÖHLER, W. BRUNNER, C. H. EHRLICH, H. HUBER and K. REIMER, *Microelectronic Eng.* **21** (1993) 159.
27. B. LÖCHEL, A. MACIOSZEK, J. STRUBE and H. HUBER, *Microelectronic Eng.* **11** (1990) 279.
28. G. FUHR, T. MÜLLER, TH. SCHNELLE, R. HAGEDORN, A. VOIGT, S. FIEDLER, W. M. ARNOLD, U. ZIMMERMANN, B. WAGNER and A. HEUBERGER, *Naturwissenschaften* **81** (1994) 528.
29. G. A. DUNN and J. P. HEATH, *Exp. Cell Res.* **101** (1976) 1.
30. D. M. BRUNETTE, *ibid.* **164** (1986) 11.
31. G. FUHR and S. G. SHIRLEY, in Proceedings of Micro Mechanics Europe MME '94, Pisa, Italy (1994) p. 164.

*Received 3 January
and accepted 29 March 1995*